

This article was downloaded by:

On: 17 January 2011

Access details: *Access Details: Free Access*

Publisher *Taylor & Francis*

Informa Ltd Registered in England and Wales Registered Number: 1072954 Registered office: Mortimer House, 37-41 Mortimer Street, London W1T 3JH, UK



International Journal of Environmental Analytical Chemistry

Publication details, including instructions for authors and subscription information:

<http://www.informaworld.com/smpp/title~content=t713640455>

Determination of ultratrace lead with bismuth film electrodes based on magneto-voltammetry

Yanping Gao^a; Wanzhi Wei^a; Xiaohua Gao^a; Jinxiang Zeng^a; Jian Yin^a

^a State Key Laboratory of Chemical, Biological Sensing Technologies & Chemometrics, Hunan University, Changsha 410082, PR China

To cite this Article Gao, Yanping , Wei, Wanzhi , Gao, Xiaohua , Zeng, Jinxiang and Yin, Jian(2007) 'Determination of ultratrace lead with bismuth film electrodes based on magneto-voltammetry', *International Journal of Environmental Analytical Chemistry*, 87: 7, 521 – 533

To link to this Article: DOI: 10.1080/03067310701218932

URL: <http://dx.doi.org/10.1080/03067310701218932>

PLEASE SCROLL DOWN FOR ARTICLE

Full terms and conditions of use: <http://www.informaworld.com/terms-and-conditions-of-access.pdf>

This article may be used for research, teaching and private study purposes. Any substantial or systematic reproduction, re-distribution, re-selling, loan or sub-licensing, systematic supply or distribution in any form to anyone is expressly forbidden.

The publisher does not give any warranty express or implied or make any representation that the contents will be complete or accurate or up to date. The accuracy of any instructions, formulae and drug doses should be independently verified with primary sources. The publisher shall not be liable for any loss, actions, claims, proceedings, demand or costs or damages whatsoever or howsoever caused arising directly or indirectly in connection with or arising out of the use of this material.

Determination of ultratrace lead with bismuth film electrodes based on magneto-voltammetry

YANPING GAO, WANZHI WEI*, XIAOHUA GAO,
JINXIANG ZENG and JIAN YIN

State Key Laboratory of Chemical, Biological Sensing Technologies & Chemometrics,
Hunan University, Changsha 410082, PR China

(Received 1 September 2006; in final form 15 January 2007)

A novel method for the determination of Pb^{2+} with bismuth film electrodes (BFEs) based on magneto-voltammetry was investigated. In the presence of a 0.6 T external magnetic field, square wave voltammetry of Pb^{2+} was performed with BFEs. A high concentration of Fe^{3+} was added to the analytes to generate a large cathodic current during the preconcentration step. A Lorentz force from the flux of net current through the magnetic field resulted in convection. Then, more Pb^{2+} deposited onto the electrode and larger stripping peak currents were observed. BFEs that were prepared by simultaneously depositing the bismuth and Pb^{2+} on an electrode offered a mercury-free environment for this determination. This method exhibits a high sensitivity of $4.61 \mu\text{A} \mu\text{M}^{-1}$ for Pb^{2+} over the 1×10^{-8} to 1×10^{-6} M range. A detection limit as low as 8.5×10^{-10} M was obtained with only 1-min preconcentration. The method was successfully applied to determine Pb^{2+} in real water samples.

Keywords: Magneto-voltammetry; Bismuth film electrodes; Lead; Square wave voltammetry

1. Introduction

Lead is a poisonous chemical which is widely distributed in nature and occurs in the form of inorganic or organic compounds. The presence of lead in food and water above a certain level presents a serious threat to public health, such as cancerization and hypogenesis [1]. Therefore, it is extremely important to monitor trace or ultratrace lead in the environment. Commonly, the analytical methods for the determination of lead ion are atomic absorption spectrometry (AAS) [2], inductively coupled plasma-mass spectrometry (ICP-MS) [3], X-ray fluorescence (XRF) [4]. However, these reliable techniques require expensive instrumentation and are additionally time-consuming. They cannot be used for routine in-field monitoring of a large number of samples.

*Corresponding author. Fax: +86-731-8821967. Email: weiwz2003@126.com

Electrochemical stripping analysis has been recognized as a powerful tool for the trace analysis of metal ions because of its low cost, easy operation, good sensitivity, and high selectivity [5]. The mercury film electrode (MFE) and hanging mercury drop electrode (HDME) have been widely used to detect lead due to their high sensitivity and reproducibility [6, 7]. But mercury is harmful to the environment and human bodies. Therefore, great efforts have been taken to develop mercury-free electrodes to detect lead. Honeychurch *et al.* [8] used a calixarene-modified screen-printed carbon electrode to determine lead, and an LOD of 24.1 nM was achieved with 10-min preaccumulation. Dragoe *et al.* [9] determined lead in tap water at a boron-doped diamond electrode using anodic stripping voltammetry (ASV) and obtained an LOD of 2 nM with 15-min preaccumulation. Ouangpipat *et al.* [10] applied *Pennisetum* modified carbon-paste electrodes to detect lead, and an LOD of 480 nM was obtained. Honeychurch *et al.* [11] used 1-(2-pyridylazo)-2-naphthol modified screen-printed carbon electrodes to determine lead giving an LOD of 72.3 nM. Wanekaya *et al.* [12] detected lead using overoxidized polypyrrole film and achieved an LOD of 48.2 nM. However, they suffer from long analysis times or high detection limits.

In ASV, there are many ways to enhance mass transport during the deposition step to decrease the detection limits or shorten deposition time, such as using a stirrer [13], rotating disk electrode [14], or microelectrode [15]. On the other hand, it has been shown that a magnetic field can enhance mass transport in electrochemical reactions. This effect is called the magnetohydrodynamic (MHD) effect [16–21]. The applications of MHD effect in electrochemical systems have been conducted with metal electrodeposition, which focused on the morphology [22], crystal microstructure of electrodeposited thin film [23], and kinetics [24]. However, investigations into the magnetic field effects on analytical methods are limited. A recent report investigated that redox MHD can be used to induce convection in the solution during the deposition step in linear scan ASV [25]. The induced convection enhanced the mass transport of analytes to the electrode, and then the sensitivities increased and limits of detection decreased compared to that obtained in the absence of a magnetic field. However, the plated mercury-film electrode used in this experiment is highly toxic to human bodies, and linear scan ASV selected as the stripping step led to somewhat higher detection limits (5 nM).

Bismuth film electrodes (BFEs) which involve *in situ* deposition of the bismuth film onto a suitable substrate have been shown to give a comparable performance to that of mercury films in ASV [26–32]. But bismuth with a very low toxicity is a more environmentally friendly metal compared to mercury. Furthermore, BFEs possess several other attractive properties, such as simple (*in situ*) preparation and well-defined and highly reproducible stripping peaks.

In this paper, a new method for the determination of ultratrace lead by square-wave anodic stripping voltammetry (SWASV) based on the combination of an external magnetic field and BFEs was developed. An external magnetic field of 0.6 T was used to induce solution convection, and the BFE that was *in situ* plated on a glass carbon electrode offered a mercury-free environment for the determination of lead. Additionally, the SWASV, the most sensitive and fast voltammetric method was employed to achieve a higher sensitivity in the presence of dissolved oxygen. This sensing and determining system based on magneto-voltammetry has the following advantages: no need to use stirrers, short analysis time, very low detection limit, high sensitivity and free of mercury. These are superior to those previously reported methods

based on electro-analysis [8–12, 25–30]. To the best of our knowledge, no reports have investigated this method for trace-heavy-metal analysis.

2. Experimental

2.1 Chemicals and reagents

All chemicals used were analytical reagents and used without further purification. A stock solution of 1×10^{-2} M Pb^{2+} was prepared by dissolving 0.3312 g of $\text{Pb}(\text{NO}_3)_2$ into a 1-L volumetric flask with double-distilled water. The working solutions with various concentration were prepared from this stock solution by appropriate dilution. An acetate buffer solution (0.10 M, pH 4.5) served as the supporting electrolyte. Solutions of Bi^{3+} and Fe^{3+} were prepared by dissolving their corresponding nitrate salts into acetate buffer solution. Double-distilled water was used throughout.

2.2 Apparatus

All the electrochemical measurements were performed with a CHI 440A electrochemical quartz crystal microbalance (Shanghai Chenhua Apparatus Co., Shanghai, China) in conjunction with a standard three-electrode system: a glass carbon electrode (3 mm in diameter) as working electrode, a platinum wire counter electrode, and an $\text{Ag}|\text{AgCl}|\text{KCl}$ (3 M) reference electrode (all from CH Instruments, Austin, TX). All potentials were reported with respect to the reference electrode. AAS determination was performed using a Z8000 Zeeman atomic absorption spectrometer (Hitachi).

A home-made electromagnet was used to apply an externally applied magnetic field across the electrochemical cell. The 4.5-cm-diameter magnet poles were set to a 1.8-cm gap. The working electrode was oriented vertically in the cell, so that its surface normal was perpendicular to the magnetic field. The reference electrode and the counter electrode were positioned each side of the working electrode (see figure 1). The electromagnet was powered by a DF1760SC10A power supply (Zhongce Electronics, Ningbo, China) and cooled by cycling water. The current in the power supply was adjusted to reach the desired magnetic field strength: from 0 T at 0 A to 0.6 T

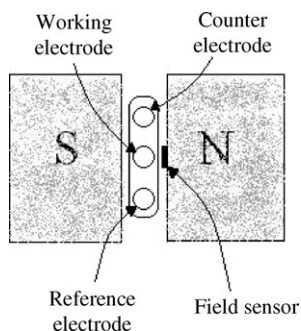


Figure 1. Experimental arrangement (top view) for measuring the voltammetric response of a glass carbon electrode in the presence of an externally applied magnetic field.

at 8 A. All the magnetic field strengths were measured with a CT3-2 Tesla meter (Shanghai Zhenhong, Shanghai, China).

2.3 Analytical procedure

The glass carbon electrode was polished with 0.3 μm and 0.05 μm alumina power until a shiny mirror-like surface was obtained, then sonicated sequentially in ethanol and double-distilled water for 2–3 min to remove trace alumina and possible contamination.

In situ bismuth films were prepared by spiking the sample with 10 μM Bi^{3+} , and the co-deposition of Bi and Pb on the surface of the electrode occurred along with the reduction of 90 mM Fe^{3+} in a magnetic field of 0.6 T. The three electrodes were immersed in a 10.00-mL electrochemical cell containing 0.1 M acetate buffer solution, and the following steps were performed:

- (1) precondition step: potential +0.6 V for 60 s was applied before each measurement to remove any possible deposits.
- (2) deposition step proceeded at -0.8 V for 60 s in a magnetic field of 0.6 T.
- (3) the square wave stripping voltammograms were recorded when sweeping from -0.8 V to -0.4 V after a 20-s quiescent time with a frequency of 12.5 Hz, amplitude of 25 mV, and potential step of 6 mV.

All experiments were carried out at room temperature.

3. Results and discussion

3.1 Effect of the orientation of the electrode relative to the magnetic field

In this paper, the ionic species in the solution are exerted on a Lorentz force in the presence of a magnetic field, and the Lorentz force density F whose magnitude and direction is defined by the right-hand rule [33–35]:

$$\vec{F} = \vec{J} \times \vec{B},$$

where, F (N m^{-3}) is the magnetic force per unit volume of solution; J (A m^{-2}) is the cathodic current generated by a high concentration of Fe^{3+} redox species due to their reduction in the deposition step; and B (T) is the magnetic field intensity. It can be seen that the Lorentz force density will become more significant at higher fields as well as higher fluxes (concentrations). With the influence of the Lorentz force, a high degree of MHD convection is generated in the solution, then more Pb^{2+} at a faster rate deposited in the bismuth thin film. Consequently, larger anodic stripping peaks are observed, and the sensitivity improves.

Figure 2 shows the direction of the Lorentz force F arising from a unit volume of the electrolyte ΔV , carrying electric current \mathbf{i} in a uniform magnetic field B . When the current vector current \mathbf{i} was orthogonal to the electrode surface, and the magnetic field B was parallel to the electrode surface, the Lorentz force F was anticipated to be the largest and parallel to the electrode surface, resulting in the largest increases in peak currents and an MHD flow of solution across the electrode surface. On the contrary,

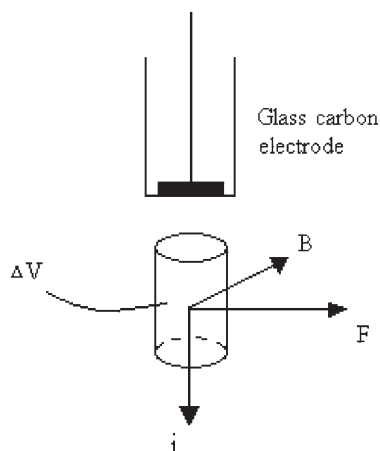


Figure 2. Direction of the Lorentz force F arising from a unit volume of the electrolyte, ΔV , carrying electric current i in a uniform magnetic field B . The magnetic field B is oriented parallel to the electrode surface. The angle between i and B is 90° .

when the current vector current i was parallel to the magnetic field B , the Lorentz force was expected to be zero, and then there was no MHD convection generated in the solution and no increase in peak currents. Such effects on electrochemical redox reactions were observed in a variety of systems [36, 37]. Therefore, the stripping peak currents were expected to reach a maximum when the current vector current i was perpendicular to the magnetic field B .

3.2 Micrograph of the Pb deposits and voltammetric behaviours of Pb^{2+} in magnetic field

Figure 3a–d shows the scanning electron micrographs of the carbon electrode prepared in the absence of Fe^{3+} and magnetic field and with 90-mM Fe^{3+} and a 0.6-T magnetic field, respectively. Figure 3a and b shows thin patches and/or nuclei on the carbon substrate. Figure 3c shows a layer of non-uniform film that partially covers the electrode. In figure 3d, a large number of Pb deposits can be clearly seen as a single particle or agglomerate particles covered on the large part of carbon surface. Thus, higher Pb stripping peak currents can be observed in the magnetic field.

The square-wave voltammograms of 1- μM Pb^{2+} under various conditions (magnetic field strength and Fe^{3+} concentration) were obtained in 0.1 M acetate buffer solution containing 10 μM Bi^{3+} . The corresponding curves are shown in figure 4. No obvious response can be observed in the absence of Fe^{3+} and magnetic field (curve a). When a 0.6-T magnetic field was exerted on the electrochemical cell in the absence of Fe^{3+} , there was no increase in peak current (curve b), thus indicating that there was no MHD effect generated in the analyte solution. After 90 mM Fe^{3+} was added to the testing solution in the absence of magnetic field, a slight increase in peak current was observed (curve c), which was due to a small degree of contamination of lead in the $Fe(NO_3)_3$ [16]. Surprisingly, when a magnetic field of 0.6 T was exerted on the electrochemical cell containing 90 mM Fe^{3+} , a clear enhancement of the peak current as large as 125% was observed (curve d) compared with curve a. This indicated that a great MHD convection

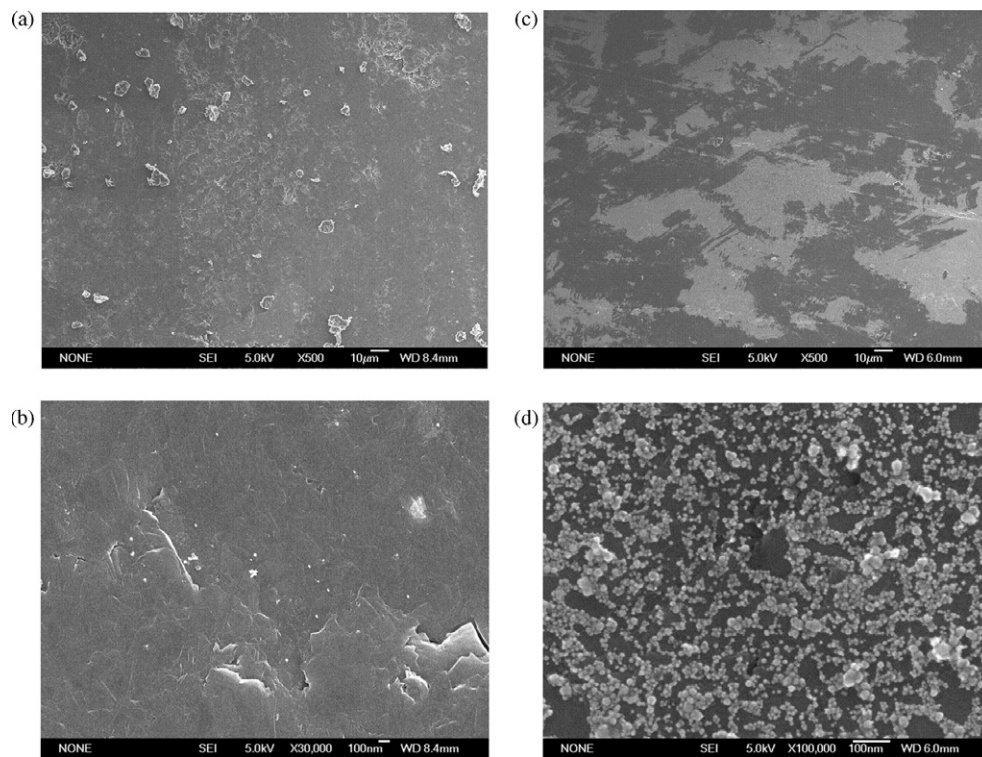


Figure 3. SEM micrographs of electrode prepared in the absence of Fe^{3+} and magnetic field (A and B) and in the presence of 90 mM Fe^{3+} and 0.6 T magnetic field (C and D). Deposition was carried out for 10 min at -0.8 V from an acetate buffer solution ($\text{pH } 4.5$) containing $10 \mu\text{M Bi}^{3+}$ and $1 \mu\text{M Pb}^{2+}$.

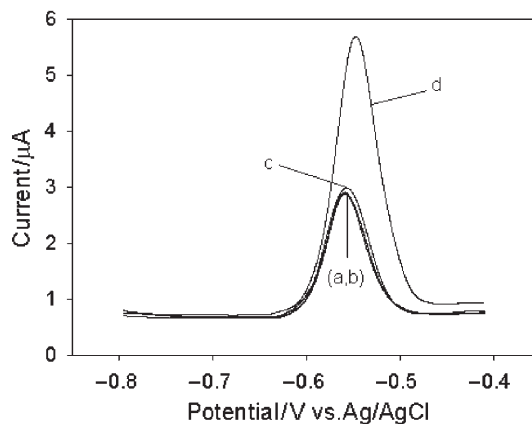


Figure 4. Comparative stripping voltammograms of $1 \mu\text{M Pb}^{2+}$ in 0.1 M acetate buffer solution containing $10 \mu\text{M Bi}^{3+}$: (a) in the absence of Fe^{3+} and magnetic field, (b) $0 \text{ mM Fe}^{3+}/0.6 \text{ T}$, (c) $90 \text{ mM Fe}^{3+}/0 \text{ T}$, and (d) $90 \text{ mM Fe}^{3+}/0.6 \text{ T}$. Deposition potential: -0.8 V ; accumulation time: 60 s; pulse amplitude: 25 mV ; frequency: 12.5 Hz ; scan increment: 6 mV .

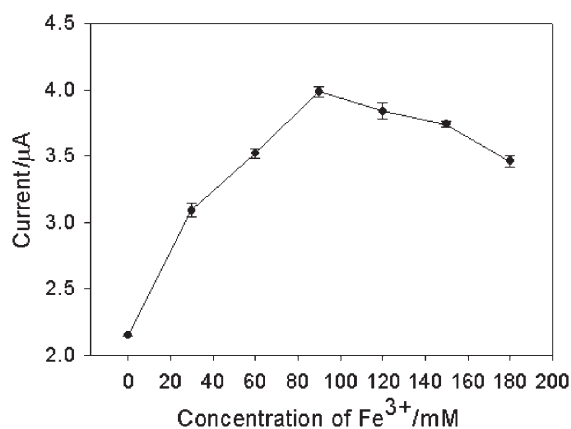


Figure 5. Effect of Fe^{3+} concentration on the stripping peak currents of Pb^{2+} at 0.6 T. Other conditions are as in figure 4. The points shown are the mean of four determinations. Error bars: standard error of the mean.

was generated in the solution, which can be interpreted as indicating that during the codeposition step, a high concentration of Fe^{3+} redox species can induce a large cathodic current, and then a large Lorentz force from the net flux of charge through the high magnetic field resulted in a high degree of MHD convection. It can be concluded that only when both the concentration of Fe^{3+} and the magnetic field were sufficiently high could a significant MHD effect be generated in the solution. Therefore, the large current response in curve d was attributed to the interaction of the Fe^{3+} redox species and the magnetic field.

3.3 Effect of the Fe^{3+} redox species concentration

The effect of different Fe^{3+} concentrations on the stripping response of $1 \mu\text{M Pb}^{2+}$ was investigated by SWASV at 0.6 T, and the results are shown in figure 5. When the Fe^{3+} concentration increased from 0 to 90 mM, the stripping peak currents increased rapidly. This can be interpreted as indicating that a higher concentration of Fe^{3+} redox species led to a higher cathodic current during the deposition step. Then, a larger magnetic force from the flux of net current through the magnetic field resulted in a greater MHD convection in the solution. More lead ions at a faster rate were deposited in the bismuth film, and then higher stripping peak currents were observed. However, when Fe^{3+} concentration was over 90 mM, the stripping peak current decreases remarkably. Therefore, the optimum Fe^{3+} concentration was chosen as 90 mM in the following experiments.

3.4 Effect of the magnetic field strength

Figure 6 shows the influence of various magnetic field strengths on the stripping peak heights of $1 \mu\text{M Pb}^{2+}$. It can be seen that an increase in the magnetic field resulted in an enhancement of stripping peak current. Comparing curve d and curve a, the peak currents increased by 63% for Pb^{2+} . When a magnetic field strength of 0.6 T was exerted on the electrochemical cell (curve g), an enhancement of the peak current as

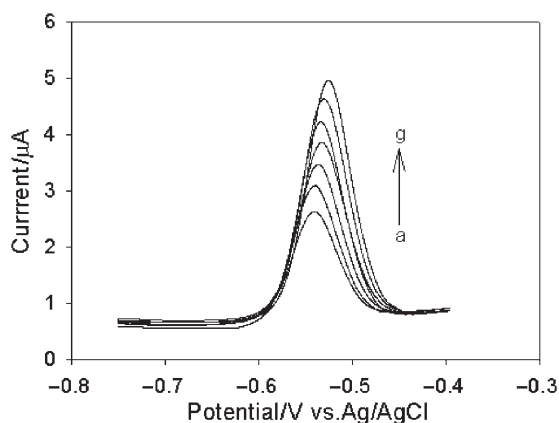


Figure 6. Voltammograms of a solution containing $1 \mu\text{M Pb}^{2+}$ at different magnetic field strengths: (a) 0, (b) 0.1, (c) 0.2, (d) 0.3, (e) 0.4, (f) 0.5, (g) 0.6 T. Other conditions are as in figure 4.

large as 118% for Pb^{2+} was observed, compared with curve a. This is mainly because an increase in magnetic field strength led to an increase in Lorentz force, resulting in a more significant MHD effect. Then, more Pb^{2+} was deposited on the electrode surface, and the stripping peak currents increased. Therefore, the magnetic field strength was chosen as 0.6 T for subsequent analytical work.

3.5 Effect of the Bi^{3+} concentration

The Bi^{3+} concentration used for *in situ* formation of the bismuth film was found to influence the height of stripping peaks of trace metals, since it controls the thickness of the Bi film [28, 30, 31]. In our study, the effect of Bi^{3+} concentration was investigated, and the results are shown in figure 7. First, the stripping peak currents of Pb^{2+} clearly increased with increasing Bi^{3+} concentration from 1 to $10 \mu\text{M}$, and then decreased from 10 to $40 \mu\text{M}$. This may be due to the formation of an alloy of lead with bismuth in the presence of a low concentration of Bi^{3+} [27]. However, an excess Bi^{3+} concentration over $10 \mu\text{M}$ can result in multilayer deposition of Bi, which was not favourable for Bi adhesion on the electrode surface [32]. Hence, the $10 \mu\text{M Bi}^{3+}$ concentration was selected for further determination.

3.6 Effects of deposition time and deposition potential

The effects of deposition time and deposition potential on the sensitivity of Pb^{2+} were investigated. SWASV of $1 \mu\text{M Pb}^{2+}$ was performed with deposition times of 10–120 s and deposition potential of -0.6 to -1.0 V . In figure 8, under a fixed deposition potential of -0.8 V , it can be seen that the response increased rapidly with deposition time up to 60 s; however, this increased slowly over 60 s. Therefore, a moderate deposition time of 60 s was selected. On the other hand, with 60-s deposition of Pb^{2+} , the peak current was found to be at a maximum for a deposition potential of -0.8 V (figure 9). Thus, a deposition potential of -0.8 V was selected in all of the experiments.

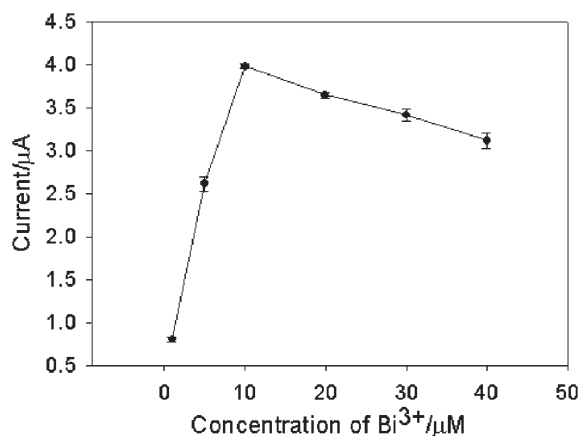


Figure 7. Effect of Bi^{3+} concentration on the SWASV peak heights of $1 \mu\text{M Pb}^{2+}$ at 0.6 T. Other conditions are as in figure 4. The points shown are the mean of four determinations. Error bars: standard error of the mean.

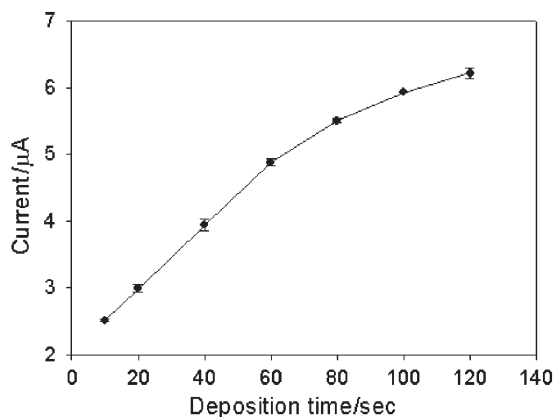


Figure 8. Effect of the deposition time on the SWASV peak heights of $1 \mu\text{M Pb}^{2+}$ at 0.6 T. Other conditions are as in figure 4. The points shown are the mean of four determinations. Error bars: standard error of the mean.

3.7 Effect of the square-wave parameters

The square-wave parameters affecting the response were frequency, pulse amplitude, and scan increment, and were investigated in 0.1 M acetate buffer solution containing $1 \mu\text{M Pb}^{2+}$. The effect of the frequency was studied from 5 to 40 Hz, and the effect of the scan increment was investigated between 1 and 9 mV. The position of the peak shifted to the anodic direction with increasing frequency or scan increment. The peak currents increased as the frequency increased. However, the peaks became ill-defined at frequencies higher than 12.5 Hz. Thus, 12.5 Hz was chosen as the optimum frequency in the measurements. The peak heights of Pb^{2+} increased with increasing scan increments up to 6 mV. Thus, the optimum scan increment was selected as 6 mV. The effect of pulse amplitude was studied from 10 to 50 mV. The position of peak shifted to the cathodic

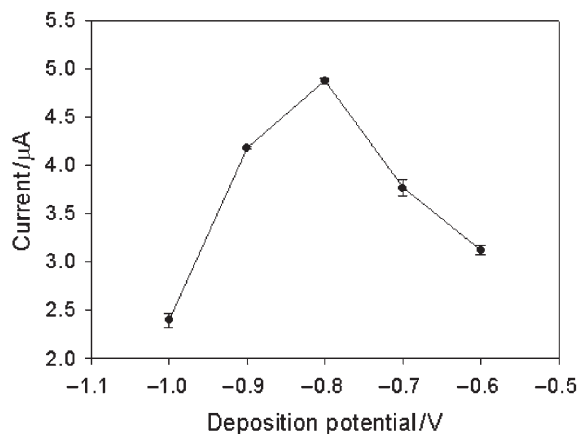


Figure 9. Effect of the deposition potential on the SWASV peak heights of $1\ \mu\text{M}\ \text{Pb}^{2+}$ at 0.6 T. Other conditions are as in figure 4. The points shown are the mean of four determinations. Error bars: standard error of the mean.

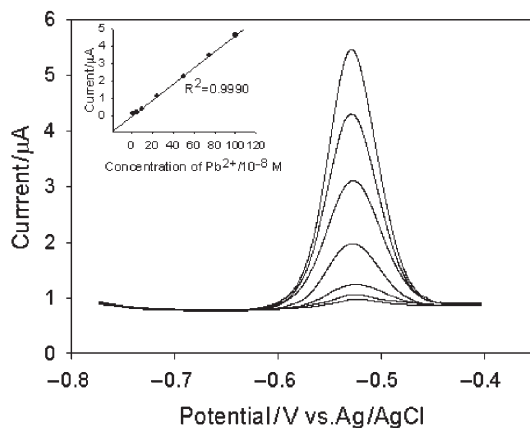


Figure 10. SWASV and the respective calibration curves of Pb^{2+} in 0.1 M acetate buffer solution containing 90 mM Fe^{3+} and $10\ \mu\text{M}\ \text{Bi}^{3+}$ at 0.6 T. Voltammograms from bottom to top are 0.01, 0.05, 0.1, 0.25, 0.5, 0.75, $1\ \mu\text{M}\ \text{Pb}^{2+}$. Deposition potential: $-0.8\ \text{V}$; accumulation time: 60 s; pulse amplitude: 25 mV; frequency: 12.5 Hz; scan increment: 6 mV. The points shown are the mean of four determinations. Error bars: standard error of the mean.

direction, and the stripping peak currents increased with increasing pulse amplitude. However, the background also increased dramatically. Therefore, a moderate pulse amplitude of 25 mV was selected for subsequent experiments.

3.8 Calibration plots and LODs of Pb^{2+}

Figure 10 showed stripping voltammograms for the detection of Pb^{2+} in 0.1 M acetate buffer solution containing 90 mM Fe^{3+} and $10\ \mu\text{M}\ \text{Bi}^{3+}$ in the concentration range of 1×10^{-8} to $1 \times 10^{-6}\ \text{M}$. All calibration experiments were performed at 0.6 T using

SWASV with Pb^{2+} deposition for 60 s at -0.8 V. As can be seen, the peak currents show an excellent linear dependence on lead concentration in bulk solution, yielding straight-line equations and i_p (μA) = $4.61 [\text{Pb}^{2+}]$ ($\mu\text{A } \mu\text{M}^{-1}$) $- 0.0004$ (μA), with a good correlation coefficient ($R^2 = 0.9990$) (see inset, figure 10). The detection limit was estimated from the signal-to-noise ($S/N = 3$) and was 8.5×10^{-10} M with a 60-s preconcentration time. Thus, quantitative determination of Pb^{2+} was possible with magneto-voltammetry.

The relative standard deviations (RSDs) of 10 measurements of 5×10^{-7} M Pb^{2+} were 4.5% at the same electrode, respectively. This result suggests that the determination of metal ions with BFE based on the magneto-voltammetry shows an excellent reproducibility.

3.9 Interferences

The possible interference of some coexisting metal ions is summarized in table 1. The results suggest that in the presence of 100-fold excess of other cations, the signal deviations of 5×10^{-7} M Pb^{2+} were no larger than 5%. Only a high concentration of Cu^{2+} (1×10^{-4} mol L $^{-1}$) was found to interfere considerably with the determination, which was because there was a competition between electrodeposited copper and bismuth for surface sites [27]. Then, in the presence of a high concentration of Cu^{2+} , a thinner bismuth film was formed, and then the peak current of Pb^{2+} drastically decreased.

3.10 Application to a real matrix

In order to illustrate its application in real sample analysis, magneto-voltammetry was finally used to detect Pb^{2+} in real water samples. Sample 1 was collected from the Powder Metallurgic Factory of Zhongnan University (Changsha, China), and sample 2 was from Xiangjiang River (Changsha, China). The two samples had no obvious suspended materials. Each sample was diluted with 0.2 M acetate buffer solution containing 180 mM Fe^{3+} and 20 μM Bi^{3+} (1:1), and then directly added into the

Table 1. Influence of interfering ions on the stripping peak currents of 5×10^{-7} M Pb^{2+} .

Interfering ions	Concentration (mol L $^{-1}$)	Signal change (%)
K^+	1×10^{-3}	+0.4
Ca^{2+}	1×10^{-3}	+1.1
Al^{3+}	1×10^{-3}	+1.2
Mg^{2+}	1×10^{-3}	+0.8
Fe^{2+}	1×10^{-3}	+2.9
Ni^{2+}	1×10^{-3}	-4.2
Co^{2+}	1×10^{-3}	-3.9
Mn^{2+}	1×10^{-3}	-2.1
Zn^{2+}	1×10^{-4}	-3.7
Cd^{2+}	1×10^{-4}	-4.8
Ag^+	1×10^{-4}	+2.6
Cu^{2+}	1×10^{-4}	-36.3

Table 2. Results of the determination of Pb^{2+} in real water samples with magneto-voltammetry and AAS.

Sample	Detected by this method (nM) ^a	Detected by AAS (nM)
1	32.5 ± 0.05	31.2
2	14.6 ± 0.08	12.7

^aMean of five-determination \pm relative standard deviation.

detection cell without any other pretreatment. In order to testify to the accuracy of this method, the same determinations were also carried out by AAS. The comparative results are shown in table 2 and suggest that there is a satisfactory agreement between the two techniques. Therefore, magneto-voltammetry shows great promise for practical sample analysis.

4. Conclusions

A sensitive method for the ultratrace determination of Pb^{2+} with bismuth film electrodes (BFEs) based on magneto-voltammetry was investigated. In the presence of an external magnetic field of 0.6 T and Fe^{3+} 90 mM redox species, an enhancement as large as 125% for the peak current was observed in SWASV with BFEs. The environmentally friendly BFEs have been shown to offer a high-quality stripping performance for determination of lead. This method has several outstanding analytical features. For example, it does not require any stirrers, and it has a short analysis time, very low detection limits, excellent reproducibility, and a high sensitivity. It also does not involve the use of mercury, and it yields reliable results. Magneto-voltammetry shows great promise in chemical and biological sensing.

Acknowledgement

This work was supported by the Specialized Research Fund for the Doctoral Program of Higher Education (SRFDP).

References

- [1] Z.J. Li, Y.L. Yang, J. Tang, J.M. Pan. *Talanta*, **60**, 123 (2003).
- [2] S. Saracoglu, M. Soyak, D.S. Kacar Peker, L. Elci, W.N.L. dos Santos, V.A. Lemos, S.L.C. Ferreira. *Anal. Chim. Acta*, **575**, 133 (2006).
- [3] C.D. Palmer, M.E. Lewis Jr, C.M. Geraghty, F. Barbosa Jr, P.J. Parsons. *Spectrochim. Acta B*, **61**, 980 (2006).
- [4] M. Mages, W. Tümping jun., A. Veen, M. Baborowski. *Spectrochim. Acta B*, **61**, 1146 (2006).
- [5] P.J.S. Barbeira, L.H. Mazo, N.R. Stradiotto. *Analyst*, **120**, 1647 (1995).
- [6] C.P. Silva, H.M. Carapuça. *Electrochim. Acta*, **52**, 1182 (2006).
- [7] C. Locatelli. *Electrochim. Acta*, **52**, 614 (2006).

- [8] K.C. Honeychurch, J.P. Hart, D.C. Cowell, D.W.M. Arrigan. *Sensor. Actuat. B*, **77**, 642 (2001).
- [9] D. Dragoe, N. Spătaru, R. Kawasaki, A. Manivannan, T. Spătaru, D.A. Tryk, A. Fujishima. *Electrochim. Acta*, **51**, 2437 (2006).
- [10] W. Ouangpipat, T. Lelasattarathkul, C. Dongduen, S. Liawruangrath. *Talanta*, **61**, 455 (2003).
- [11] K.C. Honeychurch, J.P. Hart, D.C. Cowell. *Anal. Chim. Acta*, **431**, 89 (2001).
- [12] A. Wanekaya, O.A. Sadik. *J. Electroanal. Chem.*, **537**, 135 (2002).
- [13] K.C. Honeychurch, D.M. Hawkins, J.P. Hart, D.C. Cowell. *Talanta*, **57**, 565 (2002).
- [14] C.E. Banks, A.O. Simm, R. Bowler, K. Dawes, R.G. Compton. *Anal. Chem.*, **77**, 1928 (2005).
- [15] L. Baldrianova, I. Svancara, A. Economou, S. Sotiropoulos. *Anal. Chim. Acta*, **580**, 24 (2006).
- [16] E.A. Clark, I. Fritsch. *Anal. Chem.*, **76**, 2415 (2004).
- [17] T.Z. Fahidy. *Prog. Surf. Sci.*, **68**, 155 (2001).
- [18] N. Leventis, M. Chen, X. Gao, M. Canales, P. Zhang. *J. Phys. Chem. B*, **102**, 3512 (1998).
- [19] A. Bund, S. Koehler, H.H. Kuehnlein, W. Plieth. *Electrochim. Acta*, **49**, 147 (2003).
- [20] G. Hinds, J.M.D. Coey, M.E.G. Lyons. *Electrochem. Comm.*, **3**, 215 (2001).
- [21] N. Leventis, X. Gao. *J. Phys. Chem. B*, **103**, 5832 (1999).
- [22] I. Mogi, M. Kamiko. *J. Cryst. Growth*, **166**, 276 (1996).
- [23] H. Matsushima, T. Nohira, I. Mogi, Y. Ito. *Surf. Coat. Tech.*, **179**, 245 (2004).
- [24] O. Devos, O. Aaboubi, J. Chopart, A. Olivier. *J. Phys. Chem. A*, **104**, 1544 (2000).
- [25] E.C. Aanderson, I. Fritsch. *Anal. Chem.*, **78**, 3745 (2006).
- [26] J. Wang, J. Lu, S.B. Hocevar, P.A.M. Farias. *Anal. Chem.*, **72**, 3218 (2000).
- [27] J. Wang, J. Lu, Ü.A. Kirgöz, S.B. Hocevar, B. Ogorevc. *Anal. Chim. Acta*, **434**, 29 (2001).
- [28] D. Demetriades, A. Economou, A. Voulgaropoulos. *Anal. Chim. Acta*, **519**, 167 (2004).
- [29] L. Baldrianova, I. Svancara, M. Vlcek, A. Economou, S. Sotiropoulos. *Electrochim. Acta*, **52**, 481 (2006).
- [30] G. Kefala, A. Economou, A. Voulgaropoulos, M. Sofoniou. *Talanta*, **61**, 603 (2003).
- [31] A. Charalambous, A. Economou. *Anal. Chim. Acta*, **547**, 53 (2005).
- [32] Z. Guo, F. Feng, Y. Hou, N. Jaffrezic-Renault. *Talanta*, **65**, 1052 (2005).
- [33] S.R. Ragsdale, K.M. Grant, H.S. White. *J. Am. Chem. Soc.*, **120**, 13461 (1998).
- [34] Y. Yang, K.M. Grant, H.S. White, S. Chen. *Langmuir*, **19**, 9446 (2003).
- [35] K.M. Grant, J.W. Hemmert, H.S. White. *J. Electroanal. Chem.*, **500**, 95 (2001).
- [36] J. Lee, S.R. Ragsdale, X. Gao, H.S. White. *J. Electroanal. Chem.*, **422**, 169 (1997).
- [37] S.R. Ragsdale, J. Lee, X. Gao, H.S. White. *J. Phys. Chem.*, **100**, 5913 (1996).